Analysis of a Coplanar Parasitically Coupled Patch Antenna Using CMA and CMT

SAND2020-8622C

John Borchardt
Advanced RF Applications Dept.
Sandia National Laboratories
Albuquerque, NM, USA
jjborch@sandia.gov

***Abstract*—The impedance bandwidth of a microstrip patch antenna may be increased by additional resonances in the antenna structure. This work uses Characteristic Mode Analysis to show that a text book coplanar parasitically coupled patch design operates in this manner and that Coupled Mode Theory governs its operation.**

Keywords—Characteristic mode analysis, coupled mode theory, coplanar parasitically coupled patch antenna.

I. Introduction

The impedance bandwidth (BW) of a microstrip patch antenna may be increased by additional resonances in the antenna structure. This paper uses Characteristic Mode Analysis (CMA) to show that a coplanar parasitically coupled patch [1] operates in this manner and that its behavior is well-modeled by Coupled Mode Theory (CMT).

CMA [2] is a modal decomposition based on the method of moments (MoM) wherein a real, orthogonal basis J_n results from $[X]\,J_n = \lambda_n\,[R]\,J_n$ where $[Z] = [R] + j[X]$ is the MoM impedance matrix and λ_n is the eigenvalue [2]. Currents driven by a source can be expressed as a sum of modes: $J_{\text{total}} = \sum_n \alpha_n J_n$ where α_n are the modal weighting coefficients (MWCs) [2]. Thus, the driven admittance of a structure is the sum of all modal admittances. CMT describes the dynamics of a system of two coupled resonators as the superposition of two coupled modes, a lower-frequency in-phase mode and a higher-frequency anti-phase mode. The coupled mode frequencies $\omega_\pm = 2\pi f_\pm$ are related to the uncoupled mode frequencies $\omega_{1,2} = 2\pi f_{1,2}$ by [3]:

$$\omega_\pm = \omega_0 \pm \sqrt{\left(\frac{\omega_2 - \omega_1}{2}\right)^2 + |K|^2} \qquad (1)$$

where $\omega_0 = (\omega_2 + \omega_1)/2 = 2\pi f_0$ and K is an un-normalized coupling coefficient.

II. Characteristic Mode Analysis

Fig. 1 shows a coplanar coupled patch structure from [1].

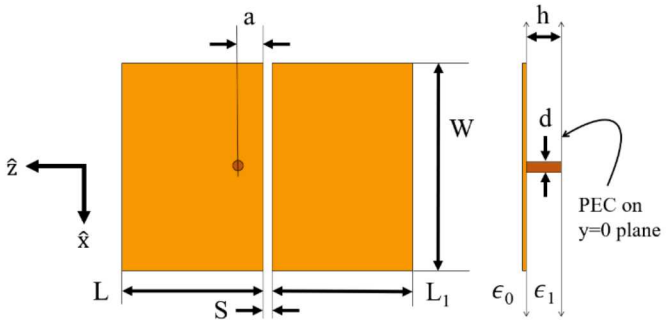

Fig. 1. Coplanar patch geometry of [1]; (W, L, L_1, S, a, d, h) = (40, 30, 29, 1, 6, 1, 1.59) mm. $\epsilon_1 = 2.55$; conductors and dielectrics are modeled as ideal.

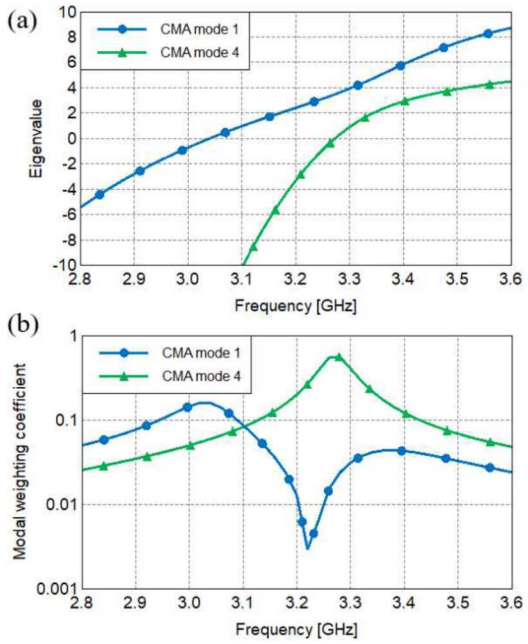

Fig. 2. (a) CMA mode 1 & 4 eigenvalues; (b) modal weighting coefficients.

A similar, early design using two parasitic patches is presented in [4], but neither [1] nor [4] perform CMA or invoke CMT. The Fig. 1 geometry is solved in FEKO [5], a MoM code with CMA. A 1V gap source located at the probe base is used for the driven solution and calculating modal weighting coefficients. Fig. 2(a) indicates modes 1 and 4 are resonant ($\lambda_n = 0$) at $f_- = 3.040$ GHz and $f_+ = 3.273$ GHz with $Q's$ of 11 and 29, respectively. The modal weighting coefficients show that only modes 1 and 4 are significantly excited; these modal weighting coefficient

Sandia National Laboratories is a multimission laboratory managed and operated by National Technology & Engineering Solutions of Sandia, LLC, a wholly owned subsidiary of Honeywell International, Inc., for the U.S. Department of Energy's National Nuclear Security Administration under contract DE-NA0003525. This paper describes objective technical results and analysis. Any subjective views or opinions that might be expressed in the paper do not necessarily represent the views of the U.S. Department of Energy or the United States Government.

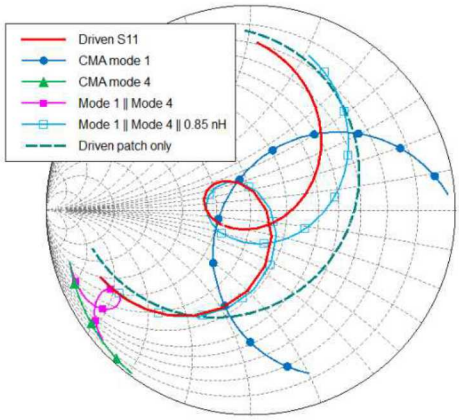

Fig. 3. The sum of mode 1 and 4 admittances captures the Smith chart loop behavior of the driven admittance; the total admittance of all other characteristic modes is well-modeled by a 0.85 nH inductor.

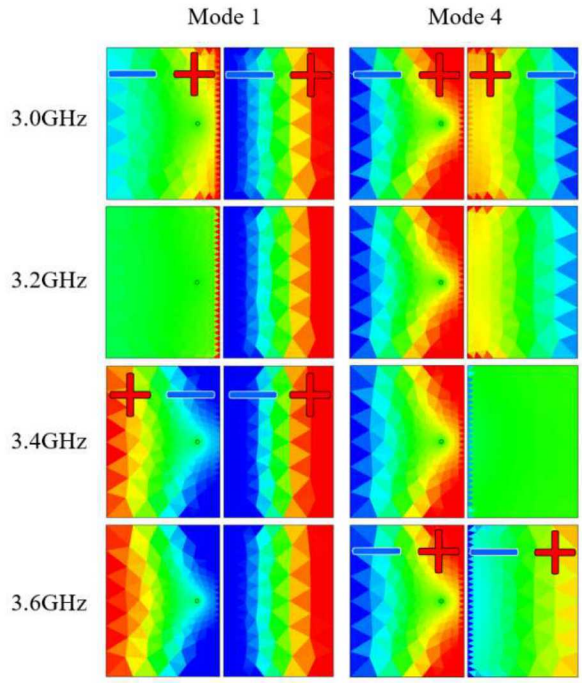

Fig. 4. Normalized modal charge distributions for CMA mode 1 (left column) and CMA mode 4 (right column) show in-phase and anti-phase relationships between the charge on the two patches. Exchange of the mode "character" (i.e., whether in-phase or anti-phase) occurs in conjunction with eigenvalue crossing avoidance [6] seen near 3.3 GHz in Fig. 2(a).

magnitudes are shown in Fig. 2(b).

Fig. 3 shows the driven admittance locus exhibits a loop about the origin. The 10 dB return loss bandwidth is about 6%, from 2.93−3.12 GHz. The parallel combination of the mode 1 and 4 admittances reproduces the Smith chart loop that is essential for broad impedance bandwidth. However, an additional shunt 0.85 nH inductance is required to closely match the driven admittance; this susceptance may be attributed to the net effect of all other characteristic modes.

Fig. 4 shows the mode 1 and 4 charge distributions, which show in-phase and anti-phase relationships between the driven and parasitic patches, e.g. at 3.0 GHz. Such relationships

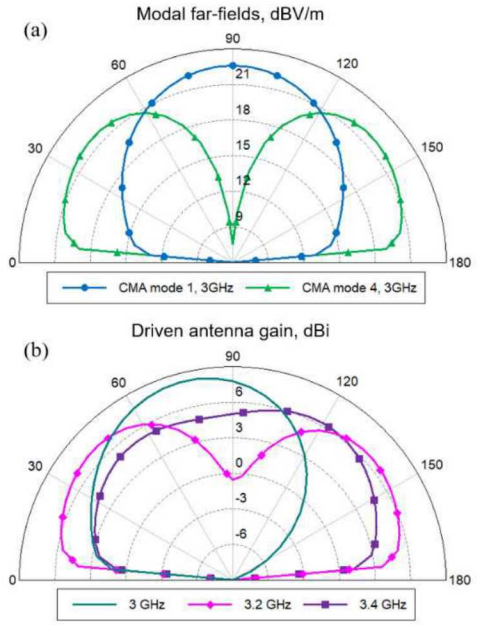

Fig. 5. (a) Mode 1 and 4 far-fields at 3.0 GHz and (b) driven problem antenna gain at 3.0, 3.2 and 3.4 GHz; all fields are co-polarized (i.e., $\hat{\theta}$-polarized) and in the E-plane (i.e., in the y-z plane).

suggest CMT is relevant to this structure. Eigenvalue crossing avoidance is observed above the impedance bandwidth near 3.3 GHz in Fig. 2(a). Near this frequency, Fig. 4 shows that modes 1 and 4 exchange "characters" near the eigenvalue crossing avoidance; i.e., mode 1 takes on anti-phase character and mode 4 takes on an in-phase character. Both eigenvalue crossing avoidance and exchange of mode characters are indicative of *coupled* characteristic modes [6].

III. Comparison with Other Multi-Modal Patches

We now compare the present case with similar analysis performed on a U-slot patch [7], an E-shaped patch [8] and a stacked patch design [9]. In cases [7] and [8], a slot in a rectangular patch radiator supports a second mode that radiates similarly to the unperturbed patch. As such, in those cases the in-phase and anti-phase modes have similar Q, their admittance loci *both* pass near the Smith chart center and *both* modes radiate approximately equally. As a result, the coupled resonances $f_{\pm}$ are approximately equally spaced about the impedance bandwidth center frequency. The present case differs in these regards; like [9], the impedance bandwidth center frequency is close to the in-phase resonance f_{-} and the anti-phase mode is seen to reactively deform the in-phase admittance locus into a loop. This improves the impedance bandwidth over the case of a single driven patch. However, in contrast to [9], the driven element here is, by itself, reasonably well matched to 50 Ω. Thus, we may interpret the coplanar parasitic element as providing a compensating impedance that extends the impedance bandwidth of the driven element.

The radiation Q of the *isolated* driven patch is 37 and *isolated* parasitic patch is 35, implying that each contribute approximately equally to radiation. Fig. 5(a) shows that this causes the anti-phase mode radiation pattern to exhibit a deep

broadside null, which is undesirable in most applications. Fig. 5(b) shows that this broadside null occurs in the driven problem around 3.2 GHz—at the upper end of the impedance bandwidth. In contrast, for the *stacked* patch geometry of [9], the isolated upper patch has a much lower radiation Q than the isolated lower patch; this implies the upper patch contributes more to radiation than the lower patch. This causes the *stacked* patch anti-phase pattern perturbation in [9] to be mild compared to that of the present case. In either case, pattern perturbations are likely the reason why semi-empirical stacked patch and coplanar coupled patch designs often locate the in-phase mode resonance near the impedance bandwidth center frequency and locate the anti-phase resonance outside of the impedance bandwidth. In short, these structures are likely *pattern* bandwidth limited, rather than being strictly impedance bandwidth limited.

IV. Coupled Mode Theory

CMA of the *isolated* driven and parasitic patches shows the *uncoupled* resonant frequencies $f_{\text{driven}} = 3.235$ GHz $\equiv f_1$ and $f_{\text{parasitic}} = 3.072$ GHz $\equiv f_2$. The unloaded $Q = 37$ of the isolated driven patch corresponds closely to the full-wave calculated 0.17 GHz 3dB return loss impedance bandwidth of the isolated driven patch (when parameter a set to 10 mm to provide a good match to 50 Ω).

A cartesian grid of modal near-fields for each of the isolated patches is calculated at their respective resonant frequencies $f_{1,2}$. The grid volume encompasses the space occupied by both elements, as shown in Fig. 6. There are 80, 52 and 60 samples in the z, x and y directions, or 249,600 total near-field points for each isolated resonator. To produce the highest quality data for near-field points close to the conducting surfaces, the mesh size was reduced to 0.5 mm and double-precision floating point was used. All these measures increase the required compute resources; however, each is necessary to achieve good results in what follows.

The normalized coupling coefficient κ between two resonators is [10]:

$$\kappa = \kappa_e + \kappa_m = \frac{\int \epsilon E_1 \circ E_2 \, dV}{\sqrt{W_{e1} W_{e2}}} + \frac{\int \mu H_1 \circ H_2 \, dV}{\sqrt{W_{m1} W_{m2}}} \qquad (2)$$

where $W_{e1,2} = \int \epsilon \left|E_{1,2}\right|^2 dV$, $W_{m1,2} = \int \mu \left|H_{1,2}\right|^2 dV$ and $E_{1,2}$ and $H_{1,2}$ are the resonant modal near-fields of the isolated resonators. We use CMA near-fields of the isolated driven and parasitic patch resonators with (2) to calculate $\kappa_e = -0.04717 - j0.01651$ and $\kappa_m = 0.00372 + j0.0169$. Thus, the total coupling κ is approximately 0.0434 (real) and is predominantly electric in nature; this satisfies our intuition regarding capacitive coupling at the open-circuit edges of two microstrip patches. Given κ, we approximate the non-normalized coupling coefficient $K \sim \kappa\omega_0/2$ as in [7]. K and $f_{1,2}$ are used in (1) to estimate coupled resonances as $f_+ = 3.270$ GHz and $f_- = 3.037$ GHz; these are within about 0.1% of the CMA-calculated coupled mode resonances of the full Fig. 1 geometry. In comparison, the isolated patch resonances $f_{1,2}$ differ from the CMT-predicted coupled resonances by greater than 1%. Thus, CMT models the behavior of this structure well, despite the very small coupling κ. Note that a small κ requires relatively high resonator Q's to produce a suitable loop in the Smith chart impedance locus [7]. This fact, together with the undesirable anti-phase mode radiation pattern, limits the ability of this structure to achieve wide bandwidth. Irrespective of this, CMT and CMA provide a valuable framework for understanding the possibilities and limitations of—as well as the relationships among—many different types of multi-modal patch geometries.

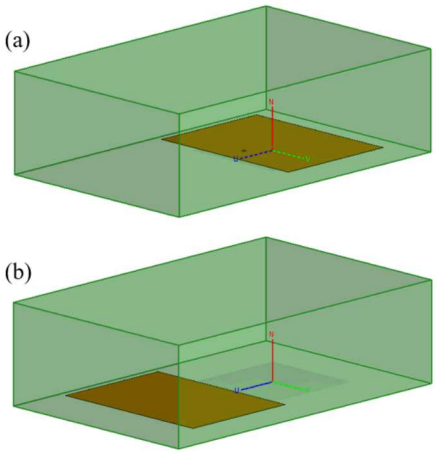

Fig. 6. Geometries and near-field volumes for calculating coupling of the isolated resonators: (a) for the driven patch and (b) for the parasitic patch.

References

[1] G. Kumar and K.P. Ray, "One Parasitic Patch" in Broadband Microstrip Antennas, Artech House, 2003, ch. 3, section 3.3.1.1, p. 91.

[2] R. Harrington and J. Mautz, "Theory of characteristic modes for conducting bodies," in IEEE Transactions on Antennas and Propagation, vol. 19, no. 5, pp. 622-628, September 1971.

[3] S. L. Chuang, "Waveguide couplers and coupled mode theory" in Physics of Optoelectronic Devices, 1st ed., Wiley, 1995, ch. 8, sec. 2.2, p. 291.

[4] G. Kumar and K. Gupta, "Broad-band microstrip antennas using additional resonators gap-coupled to the radiating edges," in IEEE Transactions on Antennas and Propagation, vol. 32, no. 12, pp. 1375-1379, December 1984.

[5] Altair Engineering, Inc. FEKO ver. 2019.2-358841 (x64) [Online] Available: https://altairhyperworks.com/product/FEKO

[6] K. R. Schab, J. M. Outwater, M. W. Young and J. T. Bernhard, "Eigenvalue Crossing Avoidance in Characteristic Modes," in IEEE Transactions on Antennas and Propagation, vol. 64, no. 7, pp. 2617-2627, July 2016.

[7] J. J. Borchardt and T. C. Lapointe, "U-Slot Patch Antenna Principle and Design Methodology Using Characteristic Mode Analysis and Coupled Mode Theory," in IEEE Access, vol. 7, pp. 109375-109385, 2019.

[8] J. Borchardt, "Analysis of an E-shaped Patch Using CMA and CMT," 2020 IEEE International Symposium on Antennas and Propagation, July 5-10, 2020 Montreal, Canada. To be published.

[9] J. Borchardt and Tyler LaPointe, "Analysis of a Stacked Patch Using CMA and CMT," 2020 IEEE International Symposium on Antennas and Propagation, July 5-10, 2020 Montreal, Canada. To be published.

[10] J. Hong, "Couplings of asynchronously tuned coupled microwave resonators," in IEE Proceedings - Microwaves, Antennas and Propagation, vol. 147, no. 5, pp. 354-358, Oct. 2000.